



# MMwave MIMO in 5G Network Analysis for Spectral Efficiency with Beamforming Based Channel Estimation

**Prof. Dharmesh Dhabliya**

Professor, Computer Engineering Department,  
Vishwakarma Institute of Information Technology,  
Pune, India  
dharmesh.dhabliya@viit.ac.in

## Abstract:

5G network has its high energy efficiency and spectrum efficiency, massive multiple-input and multiple-output (MIMO) has been envisioned as a key technology. This research work is centred on optimal method creation of energy-efficient massive MIMO methods, which is most active research technology in the communication industry. The suggested model, which takes into account a multi-cell model scenario, is a realistic method that improved spectral efficiency (SE) of huge MIMO methods. Base stations (BSs) do channel estimate based on uplink (UL) transmission using least-square (LS), element-wise MMSE, and minimum mean-squared error (MMSE) estimators. This research propose novel technique in MMwaveMIMO 5G network based spectral efficiency and channel estimation. The aim of this research is to enhance the spectral efficiency of MIMO channel using HetNets zero forcing Multiuser propagation models. The channel estimation is carried out based on beamforming using matched filter channel estimation with wide band antenna. Finally, simulation results demonstrate the high channel estimate accuracy and spectrum efficiency that the suggested systems can accomplish. Proposed technique attained sum rate of 85%, spectral efficiency of 93%, DoF of 79%, energy efficiency of 98% and detection accuracy of 96% for number of cells and sum rate of 77%, spectral efficiency of 85%, DoF of 71%, energy efficiency of 92% and detection accuracy of 95% for number of users.

**Keywords:** Massive MIMO, MMwave, 5G network, spectral efficiency, channel estimation

## 1. Introduction:-

The development of Massive MIMO systems, which have numerous transmitter and receiver antennas and great spectrum and energy efficiency, is a major driver of the adoption of the 5G network [1]. Massive MIMO networks have recently captured the attention of many academics, while models for energy augmentation, spectral efficiency, uplink and downlink transmission, and channel estimation have been scrutinised during the past ten years. On the other hand, the massive MIMO system's numerous antennas render the uplink signal assumption ineffective and complicated. In contrast to the conventional uplink detection approach, the suggested method in [2] is effective as well as attains optimal bit error rate (BER), which is based on least-square (LS) channel estimator. As a result, 5G is intended to adapt high reliability and to increase SE as well as EE with low latency [3]. Matrix inversion has been avoided by using the Richardson and Neumann series expansion (NSE) approach. Channel is also evaluated based on pilot signals that are sent by user to base stations (BS),

while massive MIMO method offers benefits of high reliability, SE and EE. For channel estimation, following methods are used: maximum likelihood, MMS technique, M-MMSE, S-MMSE, RZF, ZF, maximal ratio combining (MRC) and ZFD. However, MMSE is preferred because it has a higher spectral efficiency without adding complexity [4].

In a rich scattering propagation environment, MIMO systems' stated multiplexing advantages are achievable. Point-to-point MIMO methods can no longer give multiplexing gains over single antenna methods when there is strong correlation at either end of communication link, a strong Line-of-Sight (LoS) component. Multi-User MIMO methods (MU-MIMO) accurately abstract cellular uplink as well as downlink channel and naturally generalise single user MIMO systems. Rich scattering environments are not necessary for MU-MIMO to give higher multiplexing gain [5]. Numerous users with single antennas may connect with the base station (BS) using the same time-frequency resources in a conventional MU-MIMO system. It is





improbable that the channels of two users are substantially connected given that each user's position is random. Furthermore, multi-user diversity can help by scheduling users who are almost orthogonal to one another, preserving spatial multiplexing gains of MU-MIMO. MU-MIMO methods therefore seem to be appropriate for contemporary cellular networks. Recently, it is suggested that using a lot of antennas at the BS will enable future wireless networks to operate at high data rates as well as with enhanced EE. These systems, which have been dubbed "Massive MIMO," are thought to function in a setting where a BS outfitted with a multiplicity of [6] serves a number of customers who traditionally only use a single antenna.

The contribution of proposed technique is as follows:

1. To propose novel technique in MMwave MIMO 5G network based spectral efficiency and channel estimation
2. To enhance the spectral efficiency of MIMO channel using HetNets zero forcing Multiuser propagation models.
3. The channel estimation is carried out based on beamforming using matched filter channel estimation with wide band antenna.

## 2. Related Works:

Key objectives of 5G mobile communications networks, according to recent research activities, are to achieve 1000 times method capacity, 10 times SE, EE and data rate and 25 times average cell throughput [7]. As number of new generation devices like smartphones, tablets, and notebooks rises, so does the demand for high data rates and network dependability. The electromagnetic spectrum is a valuable but finite resource, hence massive MIMO, a high-level viewpoint technology, is used to effectively utilise that spectrum and meet demand. Massive MIMO is characterised as a method that may simultaneously serve a high number of users (UEs) by deploying a large number of smaller array antennas at BS to considerably increase beamforming and system capacity [8]. Phase noise's effects on uplink and downlink performance of massive MIMO methods have been studied in [9]–[11] as well as [12] and [13]. As a result, channel ageing can be caused by both Doppler shift and phase noise. However, only sources of channel ageing in any of these earlier experiments were either Doppler shift or phase noise. A partially connected structure (PCS) hybrid beamforming method may also be used to enhance error performance as well as average sum rate of mmWave MU-MIMO [14]. By merging beam patterns with knowledge of azimuth and elevation angles, reported PCS mechanism was

created. For next generation of wireless communication, mmWave communication was a promising method that could solve bandwidth limitation problem [15, 16]. The use of BS coordination for interference suppression is extensively studied in literature over past ten years, including works in [17]. However, these studies primarily focused on fully digital beamforming with a single RF chain behind every antenna. BS collaboration in mmWave multi-cell networks was studied in [18], but single stream communication was only mode of communication possible due to the mobile receiver's single omnidirectional antenna. The wireless industry has recently been encouraged to examine mmWave for cellular networks due to improvements in hardware design, successful outside trials, and the availability of plentiful mmWave spectrum [19]. However, due to the excessive demand on real-time signal processing for high BF gains [20], high power consumption, and cost, adopting same number of transceivers may not be practical when a large number of antennas are used to obtain superior BF gains. Therefore, it will be easier and more affordable to construct a BF structure with a lot fewer digital transceivers than total antennas. Analog BF [21], where every transceiver is connected with numerous active antennas as well as signal phase on every antenna is regulated by a network of analogue phase shifters, is an intriguing method of lowering the number of transceivers.

## 3. System Model:

This section discuss novel technique in MMwave MIMO 5G network based spectral efficiency and channel estimation. The aim of this research is to enhance the spectral efficiency of MIMO channel using HetNets zero forcing Multiuser propagation models. The channel estimation is carried out based on beamforming using matched filter channel estimation with wide band antenna.

### Channel model:

The details of a multicell massive MIMO method, including channel models, linear processing techniques, and UL and DL transmission methods, are included in this section. As shown in Figure 1, the systems depict the UL and DL MIMO transmission in cells  $j$  and  $l$ .



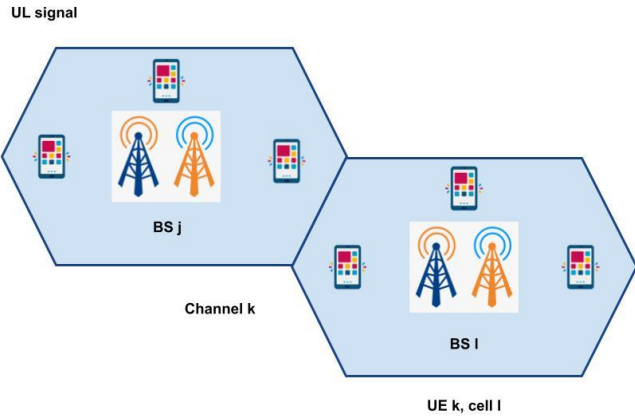


Figure 1: Illustration of UL Massive MIMO transmission in cell j and cell l.

The desired signal then changes to  $\sqrt{\rho_{UL}}V_{jk}^{UL}h_{jk}^j s_{ji}^{UL}$  due to inter- and intra-cell interference.

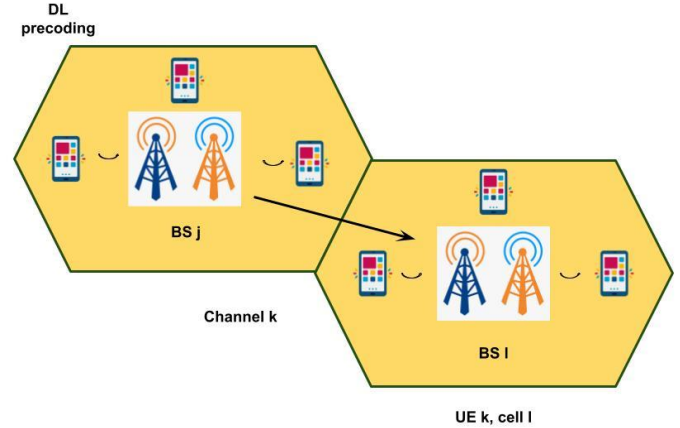


Figure 2: Illustration of DL Massive MIMO transmission in cell j and cell l

BS j transmits signal in cell l that is represented by eq. (4), in accordance with the Massive MIMO depiction for dl transmission in Figure 2:

$$x_l = \sum_{i=1}^{k_l} W_{lir_i} \quad (4)$$

where the transmit precoding vector is  $w_{lr} \in \mathbb{C}^{M_l}$ . The received signal  $y_j^{UL} \in \mathbb{C}^M$  is then simulated using equation (5):

$$y_j^{DL} = \sqrt{\rho_{DL}} \sum_{l=1}^L (h_j^{DL})^H x_l + n_j^{DL} \quad (5)$$

The symbol vector is represented by the expression  $x_l = [x_{l,1} x_{l,2} \dots x_{l,k}]$  and receiver noise additive  $n_j^{DL}$ . The SNR of DL is shown by the phrase  $\sqrt{\rho_{DL}} > 0$ . After that,  $y_j^{DL}$  can be expressed as eq. (6):

$$y_j^{DL} = \sqrt{\rho_{DL}} \sum_{l=1}^L \sum_{i=1}^{K_l} (h_{jk}^{DL})^H W_{lir_i} + n_j^{DL}$$

$$y_j^{dl} = \sqrt{\rho_{DL}} (h_{jk}^j)^H w_{jkr_{jk}} + \sqrt{\rho_{DL}} \sum_{i=1}^{K_j} (h_{jk}^j)^H W_{jir_j}$$

$$+ \sqrt{\rho_{DL}} \sum_{l=1}^L \sum_{i=1}^{K_l} (h_{jk}^{DL})^H W_{lii_{li}} + n_j^{DL}$$

$$l \neq j \quad (6)$$

In this case, the required signal for DL with intra-cell signals and inter-cell interference is  $\sqrt{\rho_{DL}} (h_{jk}^j)^H w_{jkr_{\mu k}}$ .

### HetNets zero forcing Multiuser propagation models:

We analyse a HetNet composed of BSs of various classes, which may vary in terms of deployment density  $k$ , transmit power  $P_k$ , transmit antenna count  $M_k$ , transmission technique, and users served in every resource block  $k$ . Each tier's locations are chosen at random from a homogenous PPP of independent density  $k$  that has received theoretical

Between BS j and the UE k, channel vectors  $h_{jk}$  and  $h_{lk}$  are taken into consideration in UL and DL. Desired signal, inter-cell interference, and noise have all been taken into account in the UL data transmission signal. However, a portion of the intra-cell signal has been contributed by the DL data transmission signal. User K sends information to one of the correspondence BSs at this point. Let's say that users K have transmitted symbol vector  $s_l = [s_{l,1} s_{l,2} \dots s_{l,k}]$  in the l cell. and eq. (1) can be used to represent received UL signal  $y_j^{UL} \in \mathbb{C}^M$  from users K at BSj:

$$y_j^{UL} = \sqrt{\rho_{UL}} \sum_{l=1}^L \sum_{K=1}^{K_j} h_{lk}^j s_{lk}^{UL} + n_j^{UL} \quad (1)$$

Where  $n_j^{UL}$  is an additive receiver noise denotes  $n_j^{UL} \sim \mathcal{CN}(0_{M_j}, \sigma_{UL}^2 I_{M_j})$  while  $0_{M_j}$  is zero mean and  $\sigma_{UL}^2$  is variance. Then UL signal in cell l denote  $s_{lk}^{UL} \in \mathbb{C}$  has power  $p_{UL,jk} = \mathbb{E}\{|s_{lk}^{UL}|^2\}$  and  $\rho_{UL} > 0$  means uplink SNR and U L signal  $y_j^{UL} \in \mathbb{C}^M$  is represented as eq. (2):

$$y_j^{UL} = \sqrt{\rho_{UL}} \sum_{K=1}^{K_j} h_{jk}^j s_{jk}^{UL} + \sqrt{\rho_{UL}} \sum_{l=1}^L \sum_{K=1}^{K_l} h_{li}^j s_{li}^{UL} + n_j^{UL}$$

$$i \neq j \quad (2)$$

Whereas,  $\sqrt{\rho_{UL}} \sum_{K=1}^{K_j} h_{jk}^j s_{jk}^{UL}$  is desired signal and  $\sqrt{\rho_{UL}} \sum_{l=1}^L \sum_{K=1}^{K_l} h_{li}^j s_{li}^{UL}$  is inter-cell interference. At moment of data transmission, BS designated in cell j chooses receive combining vector  $y_j^{UL} \in \mathbb{C}^M$  in order to separate desired UE signal from interferences, and is expressed as eq. (3):

$$V_{jk}^{UL} y_j^{UL} = \sqrt{\rho_{UL}} V_{jk}^{UL} h_{jk}^j s_{ji}^{UL} + \sqrt{\rho_{UL}} \sum_{i=1}^{K_j} V_{jk}^{UL} h_{jk}^j s_{ji}^{UL}$$

$$i \neq k$$

$$+ \sqrt{\rho_{UL}} \sum_{i=1}^L \sum_{i=1}^{K_l} V_{jk}^{UL} h_{jk}^j s_{ji}^{UL} + n_j^{UL}$$

$$i \neq j \quad (3)$$

and empirical support. Three multi-cell massive MIMO method is depicted in Figure 3.

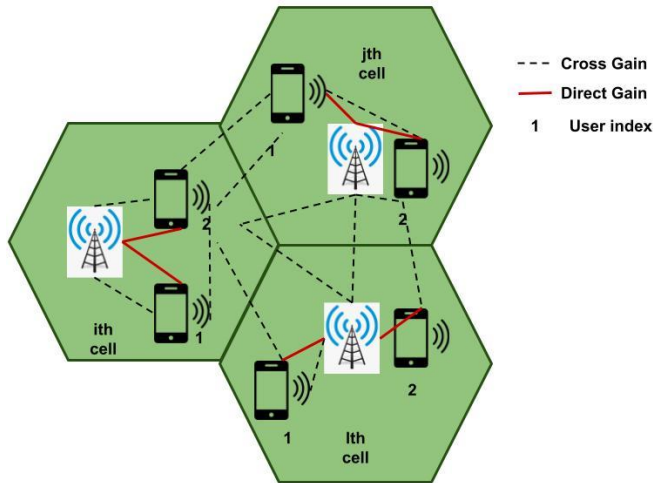


Figure 3. A multi-cell massive MIMO system

Superposition of  $K$  PPPs is used to depict the overall point process, which consists of all of the locations of BSs, as  $[k_2 K k]$ . The designation of a certain realisation of will be. It is expected that each user creates an self-regulating PPP  $u$  of density  $u$ . It is considered that every user has a single receive antenna.

Linear pre-coder  $A = c_2 \hat{H}^* (\hat{H} \hat{H}^*)^{-1}$  for zero-forcing. where  $c_2$  is a scalar constant. So, by eq (7)

$$\underline{S} = c_2 \hat{H}^* (\hat{H} \hat{H}^*)^{-1} \underline{q} \quad (7)$$

From (3) and (6), we have eq. (8)

$$\begin{aligned} \underline{\Sigma} &= c_2 \sqrt{\rho_j} H \hat{H}^* (\hat{H} \hat{H}^*)^{-1} \underline{q} + \underline{u} \\ &= c_2 \sqrt{\rho_j} \underline{q} + \left[ \underline{w} - c_2 \sqrt{\rho_j} \hat{H} \hat{H}^* (\hat{H} \hat{H}^*)^{-1} \underline{q} \right] \end{aligned} \quad (8)$$

As a result, the  $k$ -th terminal's received signal is by eq (10)

$$x_k = c_2 \sqrt{\rho_j} \varphi_k + \left[ w_k - c_2 \sqrt{\rho_j} L_{jk} \hat{H}^* (\hat{H} \hat{H}^*)^{-1} \underline{q} \right] \quad (10)$$

On the right side of the equation(10),  $x_k$  is divided into three uncorrelated terms. The signal phrase comes first. The uncorrelated noise is represented by the second term. The channel estimate error is taken into consideration in the third phrase. The analogous equation for the conjugate beamforming pre-coder contains extra terms that take into consideration cross-talk brought on by nonorthogonal channel vectors and the variance in beamforming gain. Significant SINR for  $k$ -th terminal is equal to eq(11), as can be seen from (10)

$$\text{SINR}_{et} = \frac{\text{variance}(1^{st} \text{ term})}{\text{variance}(2nd \text{ term}) + \text{variance}(3/d \text{ term})}$$

which is calculated as

$$\text{SINR}_{ed} = \frac{c_2^2 \rho_f}{1 + \frac{\rho_f}{1 + \tau_r \rho_r}} = \frac{c_2^2 \rho_f (1 + \tau_r \rho_r)}{1 + \tau_r \rho_r + \rho_f} \quad (11)$$

simply figuring out each term separately. Note that we must determine the constant scalar  $c_2$  to derive an explicit equation for significant SINR. The process for doing this is as follows. We can express equation (11), where  $s$  is the value of  $s$ , as normalising the power to satisfy constraint (12).

$$c_2 = \sqrt{\mathbb{E} \left\{ \text{Trace} (\hat{H} \hat{H}^*)^{-1} \right\}} \quad (12)$$

Since  $H = \sqrt{\frac{T.P.}{1+T_r}} Z$ , where  $Z \sim CN(0,1)_{K \times M}$ , we have by eq. (13)

$$(H H^*)^{-1} = \left( \frac{\tau_r \rho_r}{1 + \tau_r \rho_r} Z Z^* \right)^{-1} = \frac{1 + \tau_r \rho_r}{\tau_r \rho_r} (Z Z^*)^{-1} \quad (13)$$

where  $Z Z^*$  is an equation(14) based central complex Wishart matrix.

$$\mathbb{E} \{ \text{Trace} (Z Z^*)^{-1} \} = \frac{K}{M-K} \quad (14)$$

which implies by eq. (15)

$$c_2 = \sqrt{\frac{\tau_r \rho_r}{1 + \tau_r \rho_r} \cdot \frac{M-K}{K}} \quad (15)$$

Finally, combining equations (14) and (15) we obtain by eq. (16)

$$\text{SINR}_{af} = \frac{M-K}{K} \cdot \frac{\rho_f \tau_r \rho_r}{\rho_f + 1 + \tau_r \rho_r} \quad (16)$$

For aggregate of  $K$  terminals  $\mathbf{y}_m^* = \mathbf{A}_m \mathbf{s}_m + (\mathbf{U}_m^* \mathbf{U}_m)^{-1} \mathbf{U}_m^4 \mathbf{n}_m$  by eq. (17)

$$C_{\text{sum, af}} \geq K \log_2 \left( 1 + \frac{M-K}{K} \frac{\rho_f \tau_r \rho_r}{\rho_f + 1 + \tau_r \rho_r} \right) \quad (17)$$

The Multi User Detection (MUD) methodology uses the Zero Forcing (ZF) method. Due of how simple it is to use, this method is the most common. Applying the ZF approach, the choice can be written as an equation (18).

$$y_{\lambda,=}^* = \lambda_{i,m}^{\max} \sqrt{\delta_{r,m} s_{2,\dots}} + \mathbf{d}_{d,=} \mathbf{U}_m^+ \mathbf{n}_= \quad (18)$$

where,  $(\mathbf{U}_{m,m}^+ \mathbf{U}_m)^{-1} = [\mathbf{d}_{1,\infty} \mathbf{d}_{2,m} \dots \mathbf{d}_{K,m}]^T$ ,  $()^T$  is transpose operation. By using  $y_{k,m}^*$  to make the difficult decision to only take into account  $k$ th user in  $m$ th subcarrier, SNR can then be entered in (19).

$$\text{SNR}_{k,m} = \frac{(\lambda_{k,m}^{\max})^2 \delta_{k,m}}{c_{k,m} N_0} \quad (19)$$

where the spatial correlation between the  $k$ th user and other users is represented by  $c_{i,m} = |\mathbf{d}_{i,m} \mathbf{U}_m^+|_F^2$ . Keep in mind that  $F(\cdot)$  stands for the Frobenius norm. The strength of CCI in the system is correlated with this geographical connection. Because this element is unrelated to power allocation ( $\delta_{k,m}$ ), it is easier to solve optimization issue. Option  $c_{k,m}$  is 1 for the single user instance. When there are

more users,  $\kappa_{l,m}$  has a value bigger than 1. When there are numerous users present, the SNR is lower than when there is only one person. More electricity needs to be transmitted in order to maintain the same QoS when there are several users.

Assume observable combined signal at user  $u$ , which is a result of the contributions from all antenna elements across all subarrays by eqn (20),

$$z_u(n) = \sum_{l=1}^L \sum_{m=1}^M w_{l,m} h_{l,m,u}(n) * \sum_{\substack{p=1 \\ p, \text{ odd}}}^P \alpha_{l,m,p}(n) * \psi_{l,p}(n) \quad (20)$$

One may argue  $h_{l,m,u}(n) \approx h_{l,u}(n) e^{j\beta_{l,m,u}^k}$  and rephrase (20) as eq.(21) by making the typical assumption that each channel inside a single subarray is clearly correlated

$$z_u(n) \approx \sum_{l=1}^L h_{l,u}(n) * \sum_{m=1}^M w_{l,m} e^{j\beta_{l,m,u}^k} \sum_{\substack{p=1 \\ p, \text{ odd}}}^P \alpha_{l,m,p}(n) * \psi_{l,p}(n) \quad (21)$$

where particular propagation conditions and the array shape both contribute to the phase differences between the signals that make up  $e^{j\beta_{l,m,u}^k}$ . A strong case may be made for such an approximation at mmWaves, where there are often few scatterers and a dominant LOS path. The supposition naturally holds true in a pure LOS scenario in geometric channel methods with close-coupled antennas where there is a high degree of spatial correlation.  $\sum_{m=1}^M e^{j\beta_{l,m,u}^k} w_{l,m} \alpha_{l,m,p}(n)$  and  $\sum_{m=1}^M e^{j\beta_{l,m,u}^k} w_{l,m} \alpha_{l,m,p}(n)$  are highly comparable to one another. More specifically, it can be shown that

$$\sum_{m=1}^M e^{j\beta_{l,m,u}^k} w_{l,m} \alpha_{l,m,p}(n) \approx e^{j\xi_{l,u}^k} \left( \sum_{m=1}^M e^{j\beta_{l,m,u}^k} w_{l,m} \alpha_{l,m,p}(n) \right)$$

where phase  $\xi_{l,u}^k$  does not depend on  $p$ . This is due to the fact that with current PA implementation technologies and manufacturing procedures, the main cause of the interdependencies between PA samples is implementation inaccuracy. As a result, (20) and (21) may basically be rewritten as eq (22)

$$\begin{aligned} z_u^l(n) &= h_{l,u}^{\text{eff}}(n) * \sum_{\substack{p=1 \\ p, \text{ odd}}}^P \alpha_{l,p}^{\text{tot}}(n) * \psi_{l,p}(n) \\ z_{u'}^l(n) &= h_{l,u'}^{\text{eff}}(n) * \sum_{\substack{p=1 \\ p, \text{ odd}}}^P \alpha_{l,p}^{\text{tot}}(n) * \psi_{l,p}(n) \end{aligned} \quad (22)$$

where  $\alpha_{l,p}^{\text{tot}}(n) = \sum_{m=1}^M \alpha_{l,m,p}(n)$  significant channel impulse response  $h_{l,u}^{\text{eff}}$  is combined with additional user-certain constant scalar that may be common for all values of  $p$ . To do this, we replace the PA input signals in basis functions in (23), which when combined with summing over  $L$  yields, with DPD output signals, for  $l = 1, 2, \dots, L$ .

$$z_u(n) = \sum_{l=1}^L h_{l,u}^{\text{eff}}(n) * \alpha_{l,1}^{\text{tot}}(n) * \psi_{l,1}(n)$$

$$+ \sum_{l=1}^L h_{l,u}^{\text{eff}}(n) * \sum_{\substack{q=3 \\ q, \text{ odd}}}^Q \lambda_{l,q}^*(n) * \alpha_{l,1}^{\text{tot}}(n) * \psi_{l,q}(n) \quad (22)$$

$$+ \sum_{l=1}^L h_{l,u}^{\text{eff}}(n) * \sum_{\substack{p=3 \\ p, \text{ odd}}}^P \alpha_{l,p}^{\text{tot}}(n) * \psi_{l,p}(n)$$

While the remaining lines relate to nonlinear terms, the first line represents the linear signal. Next, we further assume that PA nonlinearity order  $P$  and DPD nonlinearity order  $Q$  are equivalent for the sake of notational simplicity, allowing us to rephrase (22) as eq (23)

$$\begin{aligned} \tilde{z}_u(n) &= \sum_{l=1}^L h_{l,u}^{\text{eff}}(n) * \alpha_{l,1}^{\text{tot}}(n) * \psi_{l,1}(n) + \sum_{l=1}^L h_{l,u}^{\text{eff}}(n) \\ &* \sum_{\substack{p=3 \\ p, \text{ odd}}}^P (\lambda_{l,p}^*(n) * \alpha_{l,1}^{\text{tot}}(n) + \alpha_{l,p}^{\text{tot}}(n)) * \psi_{l,p}(n). \end{aligned} \quad (23)$$

Based on (16), it is clear that the DPD filters can be selected to have a total  $l, \dots, \lambda_{l,p}(n) * \alpha_{l,1}^{\text{tot}}(n) + \alpha_{l,p}^{\text{tot}}(n) = 0$  for range of lags under consideration, hence suppressing nonlinear distortion at receiver end. This therefore more technically demonstrates that, despite all PA units being typically distinct from one another,  $L$  memory polynomial DPDs, one per subarray, may efficiently linearize  $L \times M$  various PAs. This is especially true when taking into account observable linear distortion at RX side. Formula in (16) also shows that DPD filters are independent of actual channel realisation and produce strong nonlinear distortion suppression.

### Matched filter channel estimation with wide band antenna:

The easiest method of estimating is to choose a filter with the highest cross-correlation and the least amount of noise amplification possible (24)

$$W_{\text{MF}} = \underset{w}{\text{argmax}} \frac{|E[h^H]|^2}{E[|w\eta|^2]} = \frac{\sigma_n^2}{N_p P_p} R_h S_p^H R_\eta^{-1} \quad (24)$$

The classic matched filter criterion for estimating scalar random variables, such as data detection, is generalised to random vectors in this criterion. The answer is found in Appendix A. To be consistent with the ML technique for flat uncorrelated channels, the arbitrary scalar factor in the solution is set to  $\alpha = (\sigma_n^2)/(N_p P_p)$ . The MF principle has reportedly been disregarded for channel estimation, despite being frequently utilised for channel equalisation or signal identification. The FMT signal being broadcast,  $x[n]$ , can be modified as eq (25)

$$x[n] = \sum_{i=-\infty}^{\infty} \sum_{n=0}^{M-1} s_m[i] g[n - iN] e^{j2\pi \frac{N}{M} n \frac{i}{N}} \quad (25)$$

Formula  $1/T$  yields the FMT symbol's transmission rate. Received signal is represented as  $y[n] = x[n] + h[n] + w[n]$  after channel convolution, where  $h[n]$  stands for

channel impulse response (CIR) and  $w[n]$  for additive white Gaussian noise. Aforementioned eqns expressed in following vector form for channel estimation using equation (26):

$$y = Xh + w \quad (26)$$

where  $X$  represents the pilots' reconstruction of the transmitted signal's toeplitz matrix. Single carrier channel estimate based on the matching pursuit method is thoroughly investigated, and it has been found that channel performance with the sparse estimation approach is superior to that without it. The performance of matching pursuit method in FMT sparse channel estimation has not, as far as we are aware, been examined, and this will be covered in the remaining sections of the paper. Orthogonality of base and autocorrelation function (ACF) of base are related in accordance with the properties of the Eplitz matrix. According to eq. (27), the ACF rx of FMT signal  $x$  that the pilots' reconstructions made is obtained (28)

$$\begin{aligned} r_x[k] &= \sum_{n=-\infty}^{\infty} E[x[n]x'[n-k]] \\ &= \sum_{i=0}^{N-1} \sum_{m=0}^{M-1} \sum_{r=0}^{Np_m-1} \sum_{l=0}^{M-1} E\{s_m[i]s_m^*[i]\} \\ &= N_P \sum_{m=0}^{M-1} e^{jann\frac{1}{M}} \sum_{n=-\infty}^{\infty} g[n]g^*[n-k] \\ &= A[k]r[k] \end{aligned} \quad (27)$$

$$r[k] = \sum_{n=-\infty}^{\infty} g[n]e^*[n-k] \quad (28)$$

It is considered that symbols sent on various subcarriers and at various times are uncorrelated, and that the modulated symbol's energy equals 1. The side lobes of prototype filter's ACF are small, therefore the ACF rx of the FMT signal behaves similarly to an impulse (6). This demonstrates the strong orthogonality of FMT signal's toeplitz matrix  $X$  bases. The blue solid line in Fig. 3 shows the ACF of FMT signal, and red dashed line is ACF of prototype filter. With exception of a few low sidelobes, the ACF of the FMT signal can be shown to be close to impulse, demonstrating strong orthogonality between bases of matrix  $X$ . This suggests that the matching pursuit algorithm can be used to estimate FMT sparse channels. Thus, noncausal ISI would be introduced. Let demodulation output of  $i$ th FMT symbol on  $m$ th subcarrier be as eq. (29) to avoid this.

$$z_m[i] = \sum_{n=-\infty}^{\infty} y[n]g^*[n - (i - \gamma + 1)N]e^{-j^*n\frac{1}{M^n}} \quad (29)$$

where domain of prototype filter  $g[n]$  is  $0 \leq n \leq L_g - 1$ . As a result, non-causal ISI has no longer an impact on the demodulation output. Notably, these 2 matched filtering demodulation methods are nearly identical, with exception that latter's analogous channel is delay variant of former's. (8) can be streamlined if inter-carrier interference is disregarded. Summation range for variable  $i'$  is narrowed down in accordance with the restricted domain of ACF  $r$  to

create vector form of demodulation output method. eq. (30), (31) should be satisfied by the value of  $i'$ .

$$\begin{aligned} 1 - L_g &\leq (i - \gamma + 1 - i)N - l \leq L_g - 1 \quad \forall l \in [0, L - 1] \\ &\Rightarrow i - \gamma + 1 - \frac{L_g + L}{N} \\ &\Rightarrow i - \bar{L} + 1 \leq i \leq i \end{aligned} \quad (30)$$

Where

$$\bar{L} = \gamma + \left\lfloor \frac{L_g + L - 2}{N} \right\rfloor \quad (31)$$

$L$  in the calculation above can be thought of as the corresponding FMT channel's length. The summation in (32) can then be condensed to

$$z_m[i] = \sum_{n=-\infty}^{\infty} y[n]g^*[n - (i - \gamma + 1)N]e^{-j^*n\frac{1}{M^n}} \quad (32)$$

So far, it is possible to rewrite the vector form of demodulation output method based on matched filtering as eq (33)

$$\begin{aligned} \tau_m[i] &= S_m^i R \Lambda_m h + \bar{w}_m[i] = C_m^D h + \bar{w}_m[i] \\ S_m &= [s_m[i] \cdots s_n[i - \bar{L} + 1]]_{1 \times I} \\ A &= \begin{bmatrix} 1 & \cdots & 0 \\ \vdots & & \vdots \\ 0 & \cdots & e^{-j2em\frac{1}{2}L-in} \end{bmatrix}_{L \times L} \\ &\quad + \bar{w}_m[i] \\ h &= \begin{bmatrix} h[0] \\ \vdots \\ h[L-1] \end{bmatrix}_{t \times 1} \end{aligned} \quad (33)$$

We propose function  $r$  as eq. (34) for expression simplicity.

$$r[n] = \begin{cases} r[n], & 1 - L_g \leq n \leq L_g - 1 \\ 0 & \text{otherwise} \end{cases} \quad (34)$$

After that, it is simple to obtain the subband domain FMT channel estimate model from (13). Time-frequency distribution of pilots is connected to the subband domain FMT channel estimate method in real-world applications. We get to the channel estimation model as eq. (35) without losing generality:

$$z = Ch + \bar{w} \quad (35)$$

Let  $\check{s}_k \triangleq (s_1, s_2, \dots, s_{k-1}, s_{k+1}, \dots, s_{N_t})^T$  denote a vector of transmit symbols where symbol from  $k$ th antenna is omitted. Let  $\check{p}_k$  is its square norm, i.e., by eq. (36)

$$\check{p}_k \triangleq \|\check{s}_k\|^2 \quad (36)$$

The top of this page's illustration of (9), which is the pdf conditional on  $\check{p}_k$ , expresses the pdf of real part of MF output of  $k$ th transmit antenna,  $x_k \triangleq \Re\{s_k\}$ , in terms of its input  $x_k \triangleq \Re\{s_k\}$  and all other transmit symbols  $s_k$ . For imaginary component  $y_k \triangleq \Im\{s_k\}$ , the appropriate pdf  $p_{y_k}(y | y_k = y, \check{p}_k)$  is similarly provided by (9) with  $x$  and  $x$

changed by  $y$  and  $y$ . The output from matching MF detector is given as eq. (37) starting with the  $k$ th estimated symbol

$$\begin{aligned} \hat{s}_k &= \frac{1}{\sqrt{N_r}} \mathbf{w}_k^H \mathbf{r} = \frac{1}{\sqrt{N_r}} \mathbf{w}_k^H (\mathbf{h}_k s_k + \sum_{\ell=1, \ell \neq k}^{N_t} \mathbf{h}_\ell s_\ell + \mathbf{n}) \\ &= \frac{1}{\sqrt{N_r}} \sum_{i=1}^{N_r} |h_{i,k}|^2 s_k \\ &+ \frac{1}{\sqrt{N_r}} \left\{ \sum_{i=1}^{N_r} \sum_{\ell=1, \ell \neq k}^{N_t} h_{i,k}^* h_{i,\ell} s_\ell + \sum_{i=1}^{N_r} h_{i,k}^* n_i \right\}, \end{aligned} \quad (37)$$

where  $n_k$  is total of noise and interference terms. Let's consider that, with exception of the column vector  $\mathbf{h}_k$  that identifies  $k$ th transmit antenna, which is taken to be known at detector. Additionally, the column vector  $\mathbf{s}$  is regarded as fixed. It is simple to see that output  $s_k$  is a complicated Gaussian random variable with mean determined by eq. (38) under these circumstances.

$$E\{\hat{s}_k | \mathbf{h}_k\} = \frac{1}{\sqrt{N_r}} \sum_{i=1}^{N_r} |h_{i,k}|^2 s_k = \sqrt{N_r} \alpha_k s_k \quad (38)$$

where  $\alpha_k$  is represented by the signal attenuation factor eq (39)

$$\alpha_k \triangleq \frac{1}{N_r} \sum_{i=1}^{N_r} |h_{i,k}|^2 = \frac{1}{N_r} \|\mathbf{h}_k\|^2 \quad (39)$$

and variance is represented by eq. (40)

$$\begin{aligned} \text{VAR}(\hat{s}_k | \mathbf{h}_k) &= E\{|\tilde{n}_k|^2 | \mathbf{h}_k\} \\ &= \frac{1}{N_r} \sum_{i=1}^{N_r} |h_{i,k}|^2 \sum_{\ell=1, \ell \neq k}^{N_t} E\{|h_{i,\ell}|^2\} |s_\ell|^2 \\ &\quad + \frac{1}{N_r} \sum_{i=1}^{N_r} |h_{i,k}|^2 E\{|n_i|^2\} \\ &= \frac{1}{N_r} \|\mathbf{h}_k\|^2 \left\{ \sum_{\ell=1, \ell \neq k}^{N_t} |s_\ell|^2 + N_0 \right\} = \alpha_k (\|\check{\mathbf{s}}_k\|^2 + N_0) \\ &= \alpha_k (\check{p}_k + N_0) \end{aligned} \quad (40)$$

This relies solely on  $p_k$  rather than  $s_k$ . Be aware that in equation (40),  $E\{\alpha_k\}$  is normalised so that  $E_k = 1$ . Therefore, the pdf of the output  $s_k$  is represented as eq(41), conditional on  $s_k$ ,  $p_k$ , and  $k$ .

$$p_{\hat{s}_k}(\hat{s}_k | s_k, \alpha_k, \check{p}_k) = \frac{1}{\pi \alpha_k (\check{p}_k + N_0)} e^{-\frac{|\hat{s}_k - \sqrt{N_r} \alpha_k s_k|^2}{\alpha_k (\check{p}_k + N_0)}} \quad (41)$$

Consequently, pdf for real-valued random variable  $\hat{x}_k = \Re\{\hat{s}_k \zeta'\}$  is given by eq. (42)

$$p_{\hat{x}_k}(\hat{x}_k | x_k, \alpha_k, \check{p}_k) = \frac{1}{\sqrt{\pi \alpha_k (\check{p}_k + N_0)}} e^{-\frac{(\hat{x}_k - \sqrt{N_r} \alpha_k x_k)^2}{\alpha_k (\check{p}_k + N_0)}} \quad (42)$$

Thus,  $k$  has a chi-square distribution with  $2N_r$  degrees of freedom, and its pdf is denoted by the symbol eq. (43)

$$p_{\alpha_k}(\alpha) = \frac{N_r^{N_r} e^{-N_r \alpha} \alpha^{N_r - 1}}{(N_r - 1)!} \quad (43)$$

Given by (43) at top of this page, where  $K_\mu(z)$  is modified Bessel function of second kind, is resultant pdf of (42) unconditioned on  $k$ . Using the identity provided in eq., which is valid for a positive integer  $n$  (44)

$$K_{n+\frac{1}{2}}(z) = \sqrt{\frac{\pi}{2z}} e^{-z} \sum_{r=0}^n \frac{(n+r)!}{r!(n-r)!(2z)^r} \quad (44)$$

and following some rearranging, we achieve (44). It follows exactly the same pattern for  $y_k = I s_k$  to produce the same outcome.

#### 4. Experimental Analysis:

The effectiveness of the suggested method is evaluated using simulations run on the MATLAB tool. 50 cells with different user densities are set up in a network with a  $0.5\text{km} \times 0.5\text{km}$  dimension. Local base stations are assigned to each cell, while the macro base station combines LBS communication. The MBS has a 50dBm transmit power. In Table 1, detailed simulation parameters are presented.

Table 1 Simulation Parameters and Values

Simulation Parameter	Values
Network Region	500m×500m
Path Loss Model	Rayleigh Fading
Cell Count	50
Bandwidth	180kHz
MBS	8
Path Loss Factor	3.76
Noise Power	$10^{-7}$
Users	200

Table-2 Comparative analysis of Proposed and existing technique

Cases	Techniques	Sum-rate	Spectral efficiency	DoF	Energy efficiency	Detection accuracy
Number of users	MU_MIMO	72	81	65	85	91
	EMS_MIMO	75	83	68	88	93
	MMwave_MIMO_5G_BCE	77	85	71	92	95
Number of cells	MU_MIMO	81	88	73	94	88
	EMS_MIMO	83	91	76	96	92
	MMwave_MIMO_5G_BCE	85	93	79	98	96

The above table-2 shows comparative analysis of proposed and existing technique based on number of cells and number of users. Here parametric analysis is carried out in terms of sum rate, SE, DoF, EE and detection accuracy. Existing technique compared are MU\_MIMO and EMS\_MIMO with proposed MMwave\_MIMO\_5G\_BCE. Sum rate is summation of achievable rates of multiple concurrent transmissions, for example, different users that are multiplexed. With interference limits and total power constraints, the optimization issues in MIMO with a sum rate maximisation objective seek to optimise overall system throughput. A cellular network's SE, also known as bandwidth efficiency, is comparable to highest number of bits of data that are sent to a particular number of users per second while maintaining a respectable level of service. When we talk about spectral efficiency, we often

refer to the total spectral efficiency of all transmissions within a cellular network cell. It is expressed as bit/s/Hz. You may calculate the cell throughput in bit/s by multiplying it by the bandwidth. Degree of Freedom (DoF) represents maximum number of beams can be transmitted by the base station which is equal to number of active antennas. In the limit of high SNR, DoF deals with the degrees of a communication channel or several communication channels. In the high SNR regime, this can be understood as maximum number of independent streams that are conveyed across each communication channel. The amount of bits that can be communicated over a unit of power consumption, which is often measured in bits per joule, is standard definition of energy efficiency. The electricity required to transfer data is what determines a mobile device's energy efficiency.

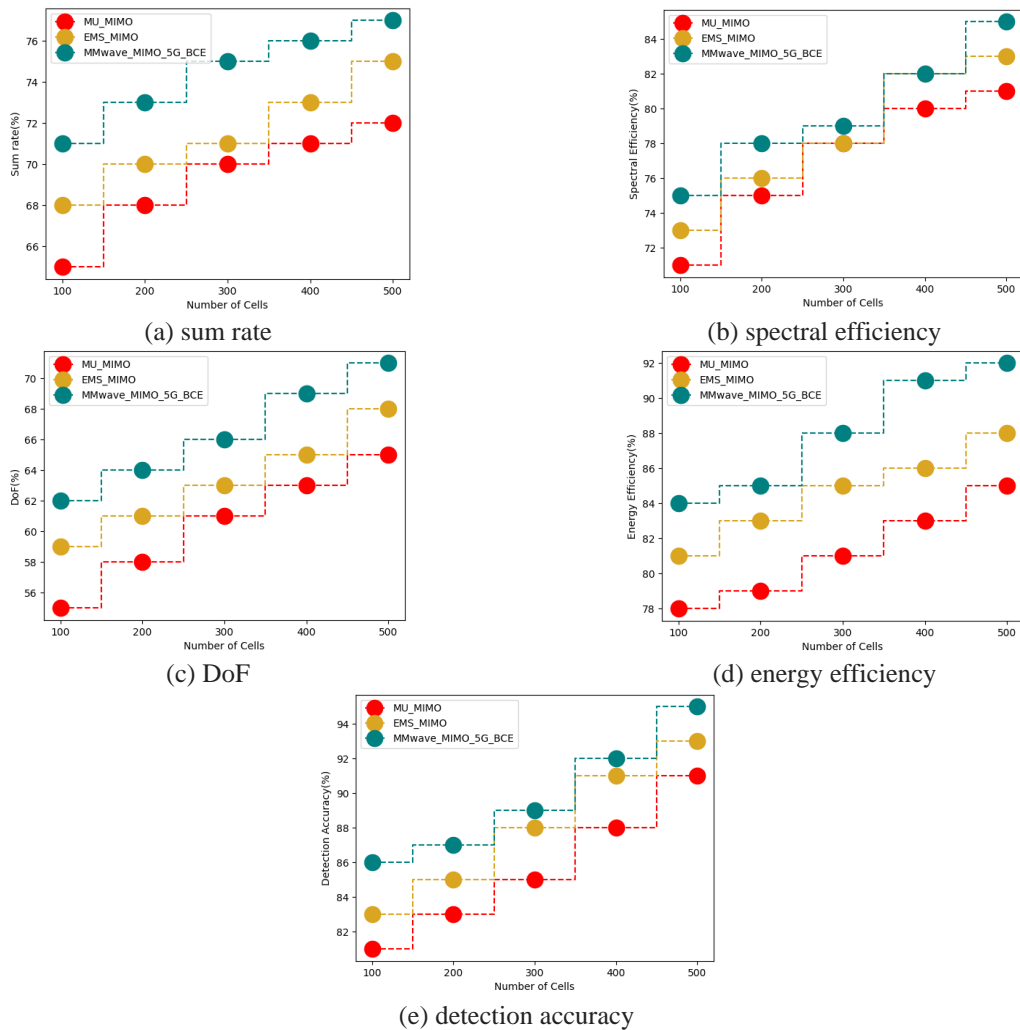


Figure-3 parametric analysis of proposed and existing technique for number of users in terms of (a) sum rate, (b) spectral efficiency, (c) DoF, (d) energy efficiency, (e) detection accuracy

From above figure-3 (a)- (e) the parametric analysis has been carried out based on number of users between proposed and existing technique. here the proposed technique attained sum rate of 77%, spectral efficiency of 85%, DoF of 71%, energy efficiency of 92% and detection accuracy of 95%. Existing technique MU\_MIMO obtained

sum rate of 72%, spectral efficiency 81%, DoF of 65%, energy efficiency of 85% and detection accuracy of 91%; EMS\_MIMO attained sum rate of 75%, spectral efficiency 83%, DoF of 68%, energy efficiency of 88% and detection accuracy of 93%.

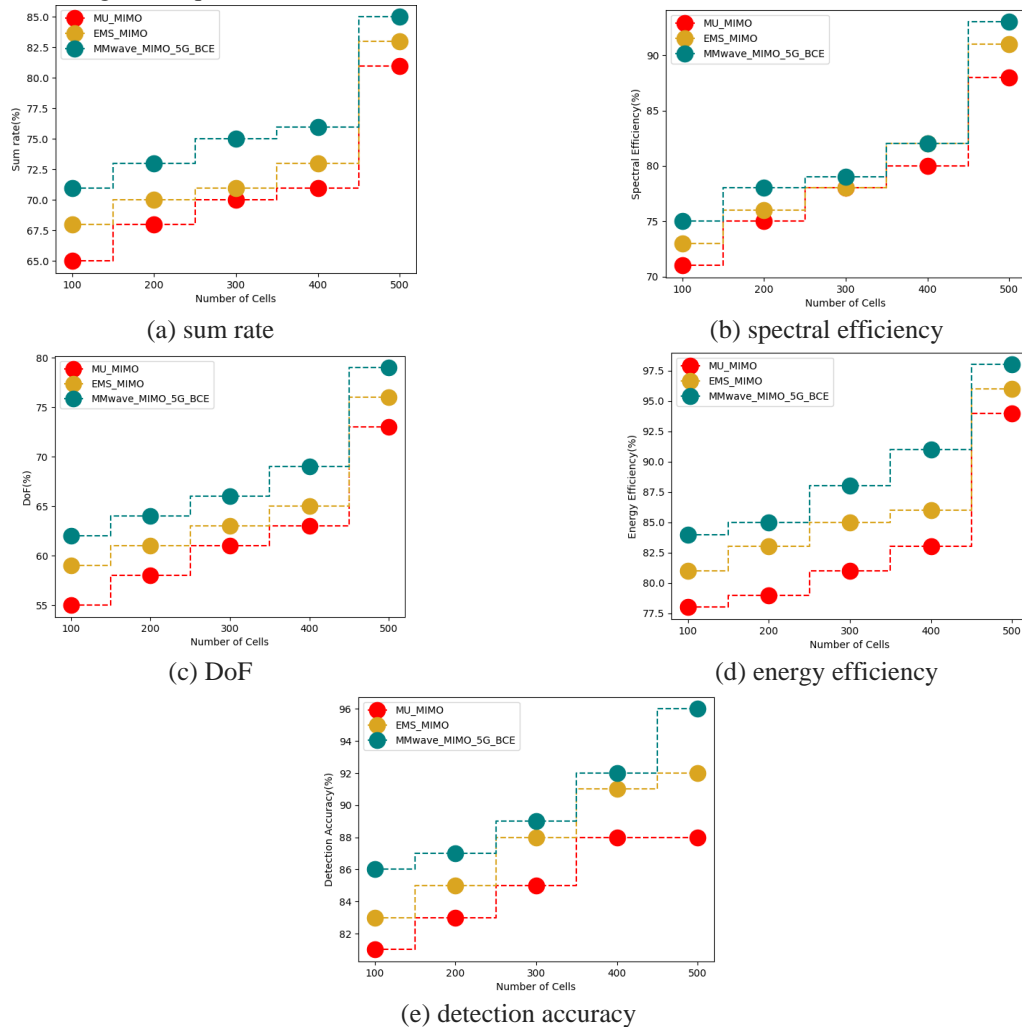


Figure-4 parametric analysis of proposed and existing technique for number of cells in terms of (a) sum rate, (b) spectral efficiency, (c) DoF, (d) energy efficiency, (e) detection accuracy

The above figure- 4 (a)- (e) shows comparative analysis between proposed and existing technique for number of cells. From the above analysis, proposed technique attained sum rate of 85%, spectral efficiency of 93%, DoF of 79%, energy efficiency of 98% and detection accuracy of 96%. While the existing technique MU\_MIMO obtained sum rate of 81%, spectral efficiency 88%, DoF of 73%, energy efficiency of 94% and detection accuracy of 88%; EMS\_MIMO attained sum rate of 83%, spectral efficiency 91%, DoF of 76%, energy efficiency of 96% and detection accuracy of 92%.

### 5. Conclusion:

In this research proposed framework designed for MMwave MIMO 5G network based spectral efficiency and channel estimation. Here the spectral efficiency has been improved using HetNets zero forcing Multiuser propagation models in MIMO channels. Then the beamforming based channel estimation is carried out using matched filter channel estimation with wide band antenna. The experimental analysis has been carried out based on number of users and number of cells where parameters analysed a sum rate, spectral efficiency, DoF, energy efficiency and detection



accuracy. proposed technique attained sum rate of 85%, spectral efficiency of 93%, DoF of 79%, energy efficiency of 98% and detection accuracy of 96% for number of cells and sum rate of 77%, spectral efficiency of 85%, DoF of 71%, energy efficiency of 92% and detection accuracy of 95% for number of users. For mmWave methods, where numerous antennas are required to give sufficient beamforming gain to enable transmission as well as reception of multiple data streams per user, fully digital beamforming, which necessitates a complete radio-frequency chain behind every antenna, is less practical. This work will be expanded upon in the future, and a thorough analysis of how cost and power usage affect system performance will be done.

### Reference:

- [1]. Uthansakul, P., & Bialkowski, M. E. (2006). An Adaptive Power and Bit Allocation Algorithm for MIMO OFDM/SDMA System Employing Zero-Forcing Multi-user Detection. *African Journal of Information & Communication Technology*, 2(2), 63-70.
- [2]. Yang, H., & Marzetta, T. L. (2013). Performance of conjugate and zero-forcing beamforming in large-scale antenna systems. *IEEE Journal on Selected Areas in Communications*, 31(2), 172-179.
- [3]. Gupta, A. K., Dhillon, H. S., Vishwanath, S., & Andrews, J. G. (2014, December). Downlink coverage probability in MIMO HetNets with flexible cell selection. In *2014 IEEE Global Communications Conference* (pp. 1534-1539). IEEE.
- [4]. Brihuega, A., Anttila, L., Abdelaziz, M., Eriksson, T., Tufvesson, F., & Valkama, M. (2020). Digital predistortion for multiuser hybrid MIMO at mmWaves. *IEEE Transactions on Signal Processing*, 68, 3603-3618.
- [5]. Qu, F., Zhang, M., Wang, Z., Qian, C., Lu, X., & Wei, Y. (2019). Sparse channel estimation for filtered multi-tone in time domain and subband domain based on matched filtering demodulation. *IET Communications*, 13(18), 2889-2894.
- [6]. Hama, Y., & Ochiai, H. (2019). Performance analysis of matched-filter detector for MIMO spatial multiplexing over Rayleigh fading channels with imperfect channel estimation. *IEEE Transactions on Communications*, 67(5), 3220-3233.
- [7]. Nalband, A. H., Sarvagya, M., & Ahmed, M. R. (2021). Spectral efficient beamforming for mmwave miso systems using deep learning techniques. *Arabian Journal for Science and Engineering*, 46(10), 9783-9795.
- [8]. Priya, T. S., Manish, K., & Prakasam, P. (2021). Hybrid beamforming for massive MIMO using rectangular antenna array model in 5G wireless networks. *Wireless Personal Communications*, 120(3), 2061-2083.
- [9]. Abdullah, Q., Salh, A., MohdShah, N. S., Abdullah, N., Audah, L., Hamzah, S. A., ... & Nordin, S. (2021). A brief survey and investigation of hybrid beamforming for millimeter waves in 5G massive MIMO systems. *arXiv preprint arXiv:2105.00180*.
- [10]. Dilli, R. (2021). Performance analysis of multi user massive MIMO hybrid beamforming systems at millimeter wave frequency bands. *Wireless Networks*, 27(3), 1925-1939.
- [11]. Kebede, T., Wondie, Y., & Steinbrunn, J. (2021, October). Performance evaluation of MillimeterWave-massive MIMO with beamforming techniques. In *2021 International Symposium on Networks, Computers and Communications (ISNCC)* (pp. 1-8). IEEE.
- [12]. Ahmed, S. A., Ayoob, S. A., & Al Janaby, A. O. (2022). Comparative Performance of mmWave 5G System for many Beamforming Methods.
- [13]. Du, J., Zhang, Y., Chen, Y., Li, X., Cheng, Y., & Rajesh, M. V. (2021). Hybrid beamforming NOMA for mmWave half-duplex UAV relay-assisted B5G/6G IoT networks. *Computer Communications*, 180, 232-242.
- [14]. Jeyakumar, P., Malar, E., Idnani, N., & Muthuchidambaramanathan, P. (2021). Large antenna array with hybrid beamforming system for 5G outdoor mobile broadband communication deployments. *Wireless Personal Communications*, 120(3), 2001-2027.
- [15]. Alsunbuli, B. N., Ismail, W., & Mahyuddin, N. M. (2021). Convolutional neural network and Kalman filter-based accurate CSI prediction for hybrid beamforming under a minimized blockage effect in millimeter-wave 5G network. *Applied Nanoscience*, 1-22.
- [16]. Cui, M., Han, W., Xu, D., Zhao, P., & Zou, W. (2021). Hybrid precoding design based on alternating optimization in mmWave massive MIMO systems aided by intelligent reflecting surface. *Computer Communications*, 180, 188-196.
- [17]. Alsunbuli, B. N., Fakhrudeen, H. F., Ismail, W., & Mahyuddin, N. M. (2022). Hybrid beamforming with relay and dual-base stations blockage mitigation in millimetre-wave 5G communication applied in (VIOT). *Computers and Electrical Engineering*, 100, 107953.
- [18]. Balti, E., & Evans, B. L. (2021). Joint beamforming and interference cancellation in mmwave wideband full-duplex systems. *arXiv preprint arXiv:2110.12266*.
- [19]. Abose, T. A., Olwal, T. O., & Hassen, M. R. (2022). Hybrid Beamforming for Millimeter Wave Massive MIMO under Multicell Multiuser Environment. *Indian Journal of Science and Technology*, 15(20), 1001-1011.
- [20]. Wang, J., Zhang, X., Shi, X., & Song, J. (2021). Higher Spectral Efficiency for mmWave MIMO: Enabling Techniques and Precoder Designs. *IEEE Communications Magazine*, 59(4), 116-122.





- 
- [21]. Feng, C., Shen, W., An, J., & Hanzo, L. (2022). Joint Hybrid and Passive RIS-Assisted Beamforming for MmWave MIMO Systems Relying on Dynamically Configured Subarrays. *IEEE Internet of Things Journal*.

